

Cross sections and transport of O^- in H_2O vapour at low pressures[★]

Vladimir Stojanović¹, Zoran Raspopović¹, Dragana Marić^{1,a}, and Zoran Lj. Petrović^{1,2}

¹ Institute of Physics, University of Belgrade, Pregrevica 118, 11080 Belgrade, Serbia

² Serbian Academy of Sciences and Arts, Belgrade, Serbia

Received 30 September 2014 / Received in final form 13 January 2015

Published online 6 March 2015 – © EDP Sciences, Società Italiana di Fisica, Springer-Verlag 2015

Abstract. The transport properties of O^- ions in water vapour drifting in DC fields were obtained by using the Monte Carlo simulation technique with the scattering cross section sets assessed on the basis of Denpoh and Nanbu's technique and available experimental data. A swarm method is applied to determine recommended cross section set. For the first time in this work we present the transport parameters for the conditions of low to moderate reduced electric fields E/N (N is gas density) accounting for the effect of non-conservative collisions. The data are applicable in the limit of low pressures where cluster formation does not affect the transport or may be applied at higher pressures together with a model of cluster formation kinetics.

1 Introduction

The interest in application of plasmas in medicine, some nanotechnologies and environmental remediation [1–5] has drawn the attention to studies of discharges in water and in proximity to water [6] although other liquids are of interest as well. Current studies show that in such systems, discharge is usually produced in water vapour either from evaporating liquid electrode or in bubbles created by an induced phase transition within the liquid. Mechanisms of breakdown in liquid without bubble formation are still under discussion [7,8]. More generally, all atmospheric discharges contain some degree of water vapour [9–12]. It is therefore of interest to determine how discharges are created in water vapour and to provide elementary transport data for the charged particles [13–17]. One of the key points must be to have an accurate knowledge of the electrical properties of water vapour and in particular of its breakdown potential [18,19]. Complicated chemistry and poor data for a range of processes of particles interacting with gas and surface require further insights and more data. In particular the data for transport and cross sections of ions are missing, especially having in mind that ions as well as electrons may have a wide range of energies, thereby affecting the profiles of electric field. In this work we analyse and provide scattering cross sections and transport coefficients of O^- ions in H_2O gas and we ex-

plore the resulting effects of non-conservative processes on the transport properties of O^- ions.

The Monte Carlo technique was applied to perform calculations of the transport parameters as well as rate coefficients in DC electric fields. We have used a Monte Carlo code that properly takes thermal collisions into account [20]. This term implies the collisions where thermal energy of targets cannot be neglected and has to be included in momentum and energy balances. Under those conditions one cannot determine the collision probabilities for projectile and for the target separately, a compound probability has to be calculated. Simplified, albeit still more complex procedures have been proposed and tested providing a proper decay of energy in the low E/N limit. The code used here is the same as in [20] and has thus passed all the relevant benchmarks [20] and has been tested in our work on several types of charged particles [21,22].

2 Cross sections and calculated transport coefficients

In what follows, we will present two sets of cross sections. The first is based on experimental data and the second on the Denpoh and Nanbu's (DN) theory [23].

2.1 The available cross section data – cross section set S1

The scattering cross sections of O^- in H_2O , measured by Hasted and Smith [24] for electron detachment (DET) and

[★] Contribution to the Topical Issue “Elementary Processes with Atoms and Molecules in Isolated and Aggregated States”, edited by Friedrich Aumayr, Bratislav Marinkovic, Stefan Matejcek, John Tanis and Kurt H. Becker.

^a e-mail: draganam@ipb.ac.rs

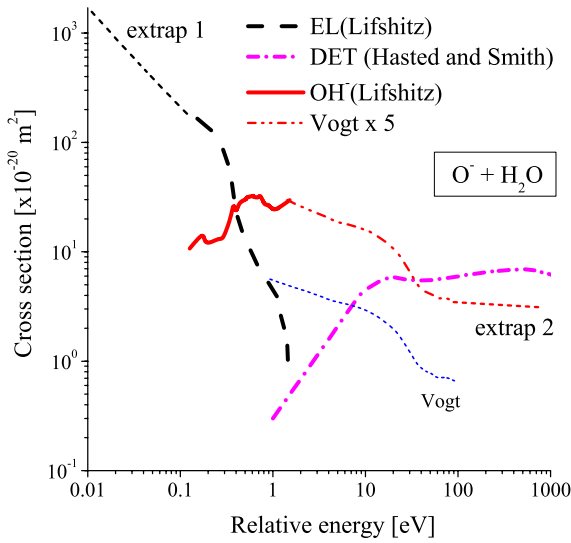


Fig. 1. Cross section set for $O^- + H_2O$ based on experimental results (S1). Cross section for the electron detachment (DET) is measured by Hasted and Smith [24], with the threshold taken from [26]. Lifshitz [25] measured cross sections for elastic scattering (EL) and for OH^- production (OH^-). The elastic cross section is extrapolated to low energies, based on the DN theory (extrap 1). Cross section for the OH^- production is extrapolated to higher energies by multiplying the results of Vogt [27] by a factor of 5 (dash-dot-dot line). (Original data of Vogt are represented by the thin dotted line.) Extension of Lifshitz cross section by using Vogt's scaled cross section up to 1 keV is indicated by "extrap 2".

Table 1. Products and the corresponding thermodynamic threshold energies Δ for the reactions $O^- + H_2O$.

No.	Products of reaction $O^- + H_2O$	Δ (eV)
1	$O^- + H_2O$ (EL)	0.
2	$OH^- + OH$	-0.36
3	$H_2O_2 + e^-$ (DET)	-0.43
	$O + H_2O + e^-$	-1.46

Lifshitz [25] for elastic scattering and OH^- formation at low energies, are shown in Figure 1 (thick lines) and processes are listed in Table 1 with their thresholds. We found them relevant for the selected domain of low O^- energies in water vapour. Preliminary results dealing with the present calculation have been presented in [28].

A cross section set S1 is completed (Fig. 1) based on these experimental data and applying extrapolations. For extrapolation at the lowest energies (dashed line labelled by "extrap 1" in Fig. 1) we have taken into account that polarisation and dipole forces are expected to be important over the energy range from 20 meV to few eV. This extrapolation is actually identical to our results for elastic scattering obtained by DN theory [23] as described in the next section.

OH^- production cross section of Lifshitz [25] was extrapolated towards high energies by using the data of Vogt [27]. The experimental data of Vogt [27] are consider-

ably lower than those of Lifshitz [25] but extend to higher energies. Note that Lifshitz explained OH^- production cross section solely through a complex formation, assuming that direct reaction is negligible, while Vogt explained his data by direct reaction only. Since both Lifshitz's cross sections [25] presented in Figure 1 are consistently measured (the same experiment), we assumed that it was reasonable to scale and connect the data of Vogt (dashed line, labelled in legend as "Vogt \times 5") to the data of Lifshitz for OH^- production (energy range from 1.5 eV to 100 eV). The scaled cross section is then extended up to 1000 eV (dashed line labelled by "extrap 2" in Fig. 1). Extrapolations to high energy were necessary to enable calculations in the tail of the ion energy distribution function, i.e. to avoid possible numerical problems to the code due to a few ions that may achieve high energies.

2.2 Cross section set based on Denpoh and Nanbu's theory (S2)

The cross sections measured by Lifshitz [25] which were the basis of the cross section set S1 were interpreted by the author as a consequence of a long lived complex formation. Thus we have calculated a cross section set by using Denpoh and Nanbu's theory (this theory is explained well in [21,23] and our procedure has been shown in detail in [21]) that assumes complex formation and is modified to treat endothermic reactions with polar molecules by the locked dipole model [29]. In DN theory a reactive collision is treated by selecting the thermodynamic threshold energy and branching ratio according to the Rice-Rampersperger-Kassel (RRK) theory [23]. We have used the data for polarizability and dipole moment of H_2O as used by Clary [30] and selected heats of formation and electron affinities from reference [31]. The threshold for electron detachment (DET) has been taken from reference [26]. The obtained cross section set was corrected to fit the reduced mobility calculated by the SACM (Statistical Adiabatic Channel Model) approximation [32] (thick lines in Fig. 2) and is labelled S2 in what follows. The zero field mobility is $K_0 = 0.984 \text{ cm}^2 \text{ V}^{-1} \text{ s}^{-1}$ at $T = 300 \text{ K}$.

Experimental elastic cross section (EL in Fig. 1) agrees well with the theoretical one up to 0.35 eV, but it falls more rapidly towards higher energies. Theoretical reactive cross section for OH^- production is about three times lower than experimental results of Lifshitz [25]. A possible variation of parameters in Denpoh and Nanbu's theory that increases this cross section worsens the other two cross sections.

It is now worth pointing again at the experimental measurements of Vogt [27] for reaction 2 in Table 1 (thin line in Fig. 2) that is in a good agreement with the present result of DN theory. On the other hand, Vogt explained his results by direct O^- excitation only, while DN theory and Lifshitz' explanation are based on complex formation. Note that the cross section for direct excitation is expected to be significantly lower than that proceeding with complex formation, so one may assume that process involving complex formation is relevant for OH^- reaction.

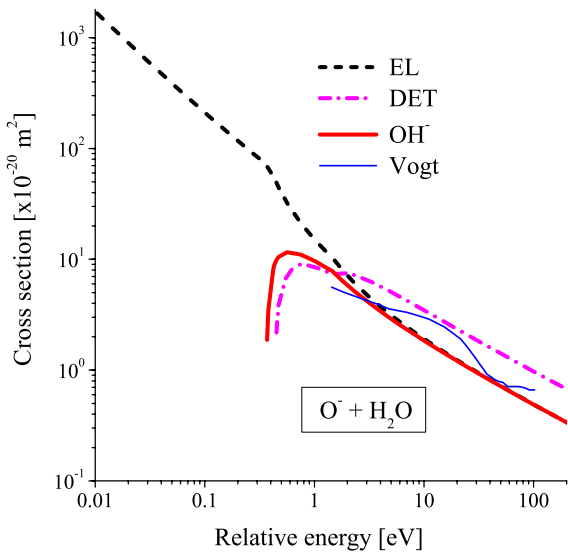


Fig. 2. Cross section set S2 for $O^- + H_2O$ based on the ND theory [23] is shown by thick lines. We show the experimental data of Vogt [27] by a thin line. EL stands for the elastic cross section, DET for detachment and OH^- for the production of OH^- .

The experimental uncertainty of the measured cross sections is as given in the papers where data were published. More importantly the discrepancies between different sources for the reaction cross section are up to an order of magnitude. The theoretical cross section is based on an approximate theory and input data that may introduce uncertainties that are difficult to assess. In both cases the best way to proceed would be to provide swarm data and normalize the set of cross sections as a whole. Only in that case one would be able to assign the uncertainty and minimize it. At the present, however, we have to use those data as better data are not available. The uncertainty introduced in transport coefficients due to our simulation is very small and for a given set of cross sections it is of the order of 0.3%.

2.3 Transport parameters

Transport parameters obtained by Monte Carlo simulation for the cross section sets S1 and S2 described above are shown in Figures 3–7. Note that these transport parameters are the only information present in the literature up to now, there are no published experimental data for the transport coefficients of O^- in pure H_2O .

Cross sections S2 fall rapidly at higher energies which is a characteristic of DN theory, so that all transport parameters are generally higher than for the case S1 at high E/N . Since at relatively high energies the total cross section S2 becomes very low and simulation may not be in equilibrium with the local electric field E/N , we show only results below 600 Td.

The endothermic (reactive) collisions affect the drift velocity at high E/N values (Fig. 3). Since the total collision frequency for endothermic reactions increases with

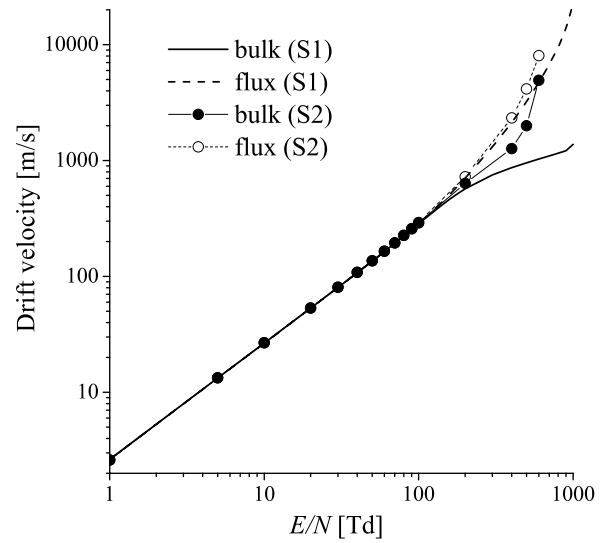


Fig. 3. Bulk and flux drift velocities for O^- ions in water vapour as a function of E/N obtained by Monte Carlo simulation at $T = 300$ K, by using cross section sets S1 and S2.

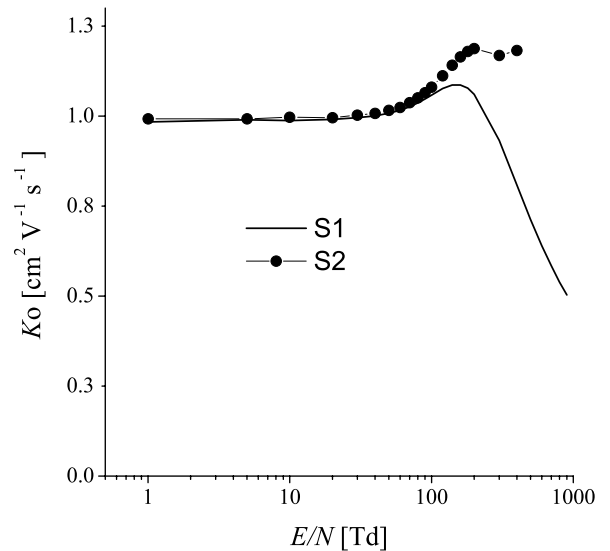


Fig. 4. Mobilities of O^- ions in water vapour as a function of E/N obtained by Monte Carlo simulation at $T = 300$ K by using cross section sets S1 and S2.

energy at high E/N thereby the dominant loss of the fast ions happens at the front of the swarm. This shifts the swarm's centre of mass towards the lower values. Thus, the bulk values (real space drift velocity $d\langle x \rangle / dt$) are lower than the flux values (velocity space drift velocity $\langle v \rangle$).

Due to the lower cross section for non-conservative processes in S2, at energies above their thresholds bulk drift velocities are closer to the flux values (as compared to the S1 results). Thus the difference between the bulk values for S1 and S2 increases with E/N (see Fig. 3). This observation indicates a possibility to distinguish between the two sets of cross sections by comparing flux and bulk

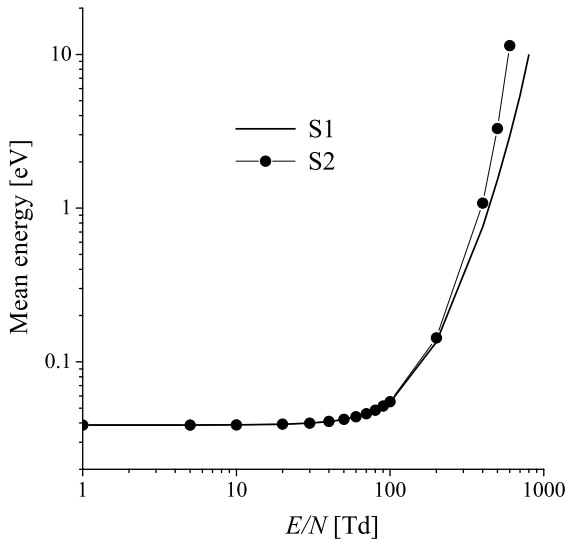


Fig. 5. Mean energies for O^- ions in water vapour as a function of E/N obtained by Monte Carlo simulation at $T = 300$ K by using cross section sets S1 and S2.

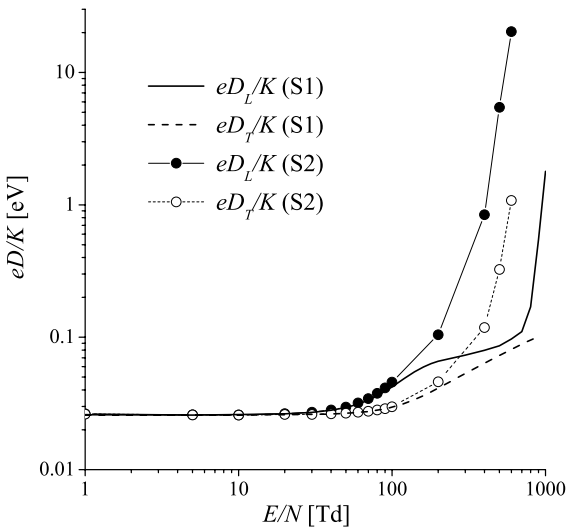


Fig. 6. Longitudinal and transverse characteristic energies for O^- ions in water vapour as a function of E/N obtained by Monte Carlo simulation at $T = 300$ K, by using cross section sets S1 and S2.

values in experiments. However, in this case there are no such measurements and it would be hard to find examples of experimental devices where such measurements could become available.

Values of the reduced mobility as a function of E/N shown in Figure 4 are sampled by using bulk drift velocities (i.e. mean velocities in real space), as those are measured in most experiments [33–35]. When the experimental or calculated data are to be used in modelling one needs to make a distinction between bulk and flux and apply the data according to the equations that are being used [34,35].

Effects of non-conservative processes become significant above 100 Td (Fig. 3). The mobility peak, repre-

senting a balance between repulsive and attractive forces appears at about 150 Td for S1 set and above 200 Td for S2 set, as seen in Figure 4.

The mean energy and the characteristic energies (longitudinal L and transverse T) are shown in Figures 5 and 6. A similar increase with E/N may be observed for diffusion coefficients, resulting in a significant increase of the characteristic energy, especially in the direction of the field (Fig. 6).

Longitudinal and transverse bulk and flux diffusion coefficients are given in Figures 7a and 7b and one should notice the very large non-conservative effects almost a reminder of the positron transport [16]. Note that the difference between the flux and bulk values of diffusion coefficients for S2 is relatively small as compared to the S1 results.

Finally, in Figure 8 we present rates for different processes for sets S1 and S2 together. Here the rate for detachment is separated from that for OH^- formation. While detachment is considerably smaller it becomes equal to OH^- formation at the highest E/N s and also one should be aware of each process separately as products are different. Comparing rates for reactions between two models, the differences between S1 and S2 results are approximately one order of magnitude different. That is consistent with the choice of the cross sections that cover well the spread of data in the literature and within the observed experimental discrepancies as reported in [25].

Formation of $O^- \cdot H_2O$ produced in three body collisions [26] is not included in our work. We assumed that processes presented in Table 1 describe O^- transport well for low pressures where binary collision regime holds and where the contribution of the three body collisions is negligible.

3 Conclusion

O^- and OH^- are the principal negative ions in discharges in water vapour. Having in mind the current interest in discharges in and close to liquids it is important to provide a complete set of cross sections that would serve as the basis for modelling such plasmas/discharges.

The present data may be expected to be valid as a complete representation of O^- kinetics for the water vapour at low enough pressures so that clustering does not affect the results. A similar procedure as employed in the model S2 may be applied to provide collisions with most buffer gases and thus cover mixtures with a small abundance of water vapour. In addition, the data may be used as the basis to help analyse the transport when clustering is important [36].

We have proposed two cross section sets based either on experimental data or on theoretical calculations (by using the Danpoh and Nanbu's theory) and those sets were used in a simulation to produce the swarm data. We would recommend the theoretical cross section set S2 as it is fully self-consistent and it agrees with elastic scattering in [25] at low energies, OH^- formation from [27] and is also consistent with the detachment cross section in [24].

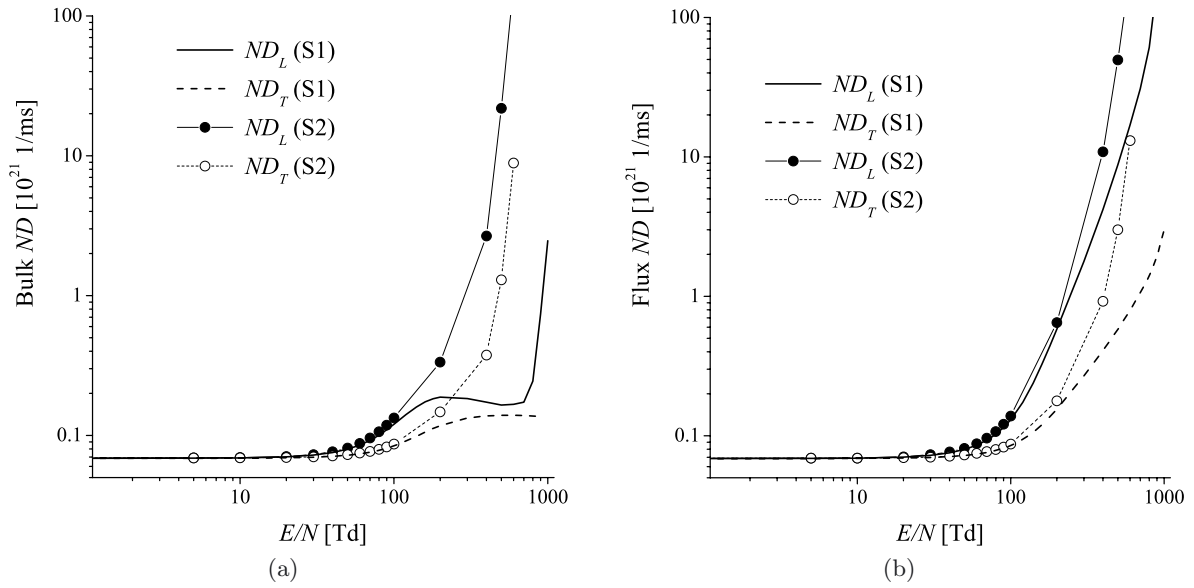


Fig. 7. Diffusion coefficients for O^- ions in water vapour as a function of E/N obtained by Monte Carlo simulation at $T = 300$ K by using cross section sets S1 and S2: (a) bulk diffusion coefficients, (b) flux diffusion coefficients.

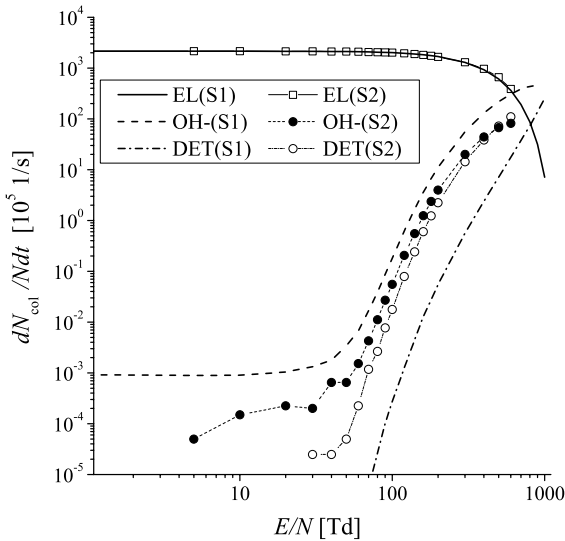


Fig. 8. Rate coefficients for collisions of O^- ions in water vapour as a function of E/N obtained by Monte Carlo simulation at $T = 300$ K, by using cross section sets S1 and S2.

This set, however, leads to very low cross sections at higher energies and thus some of the transport coefficients such as the mean energy become exceedingly high. It would be interesting to see whether a runaway of O^- ions may occur in water vapour and thus confirm such cross section shapes. Tests of runaway, however, would require exact modelling of a particular experiment (pressure, geometry, etc.) and careful consideration both in simulations and even more so in experiments. In addition one would need to establish whether some new processes at higher energies open up and also whether elastic scattering at higher

energies may have considerable contribution greater than that extrapolated from our study.

In addition to presenting the cross section and transport data we show here effects of non-conservative collisions on ion transport (that have been discussed to our knowledge for the first time for ions in [21]). Due to non-conservative cross sections that quickly become larger than the elastic scattering cross section differences between flux and bulk transport coefficients are quite large – comparable to the strongest cases observed for electrons, even positrons. Set S2 does not show such large effects as the reactive cross sections are smaller and are falling off with energy but still its non-conservative discrepancy between bulk and flux properties is significant.

Data for swarm parameters and cross sections for ions are needed for kinetic, hybrid and fluid codes and it would be essential to carry out some measurements of ion transport to be able to make these results more accurate. Realistic experiments, however, will require somewhat higher pressures to achieve local hydrodynamic equilibrium and thus could be prone to cluster formation [36].

In this paper, we showed transport properties for the O^- in water vapour which are not available in the literature. These data are needed for modelling in numerous applications where water vapour is often present in various abundances [9–12,37] thus similar cross sections for the ions in standard buffer gases would be required. Present results are also of interest for interpretation of the breakdown mechanisms [7,8,38] and early stages in the development of the discharges.

This work is partly supported by Ministry of Education, Science and Technology of Republic Serbia projects ON171037 and III410011. Z.Lj.P. is also grateful to the SASA project F155.

References

1. K.R. Stalder, G. Nersisyan, W.G. Graham, *J. Phys. D* **39**, 3457 (2006)
2. T. Hagino, H. Kondo, K. Ishikawa, H. Kano, M. Sekine, M. Hori, *Appl. Phys. Express* **5**, 035101 (2012)
3. M. Laroussi, *Plasma Processes Polym.* **2**, 391 (2005)
4. S. Lazović, N. Puač, M. Miletić, D. Pavlica, M. Jovanović, D. Bugarski, S. Mojsilović, D. Maletić, G. Malović, P. Milenković, Z.Lj. Petrović, *New J. Phys.* **12**, 083037 (2010)
5. K. Kutasi, J. Loureiro, *J. Phys. D* **40**, 5612 (2007)
6. P. Bruggeman, D. Schram, M.Á. González, R. Rego, M.G. Kong, C. Leys, *Plasma Sources Sci. Technol.* **18**, 025017 (2009)
7. I. Marinov, O. Guaitella, A. Rousseau, S.M. Starikovskaia, *Plasma Sources Sci. Technol.* **22**, 042001 (2013)
8. A. Starikovskiy, *Plasma Sources Sci. Technol.* **22**, 012001 (2013)
9. T. Murakami, K. Niemi, T. Gans, D. O'Connell, W.G. Graham, *Plasma Sources Sci. Technol.* **22**, 015003 (2013)
10. W. Van Gaens, A. Bogaerts, *J. Phys. D* **46**, 275201 (2013)
11. P. Bruggeman, C. Leys, *J. Phys. D* **42**, 053001 (2009)
12. J.D. Skalny, J. Orszagh, N.J. Mason, J.A. Rees, Y. Aranda-Gonzalvo, T.D. Whitmore, *Int. J. Mass Spectrom.* **272**, 12 (2008)
13. G. Ruíz-Vargas, M. Yousfi, J. de Urquijo, *J. Phys. D* **43**, 455201 (2010)
14. Y. Itikawa, N. Mason, *J. Phys. Chem. Ref. Data* **34**, 1 (2005)
15. R.E. Robson, R.D. White, K.F. Ness, *J. Chem. Phys.* **134**, 064319 (2011)
16. R.D. White, W. Tattersall, G. Boyle, R.E. Robson, S. Dujko, Z.Lj. Petrović, A. Banković, M.J. Brunger, J.P. Sullivan, S.J. Buckman, G. Garcia, *Appl. Radiat. Isotopes* **83**, 77 (2014)
17. J. de Urquijo, E. Basurto, A.M. Juarez, K.F. Ness, R.E. Robson, M.J. Brunger, R.D. White, *J. Chem. Phys.* **141**, 014308 (2014)
18. N. Škoro, D. Marić, G. Malović, W.G. Graham, Z.Lj. Petrović, *Phys. Rev. E* **84**, 055401(R) (2011)
19. M. Radmilović-Radenović, B. Radenović, Ž. Nikitović, Š. Matejčik, M. Klas, *Nucl. Instrum. Methods Phys. Res. B* **279**, 103 (2012)
20. Z. Ristivojević, Z.Lj. Petrović, *Plasma Sources Sci. Technol.* **21**, 035001 (2012)
21. Z.Lj. Petrović, Z.M. Raspopović, V.D. Stojanović, J.V. Jovanović, G. Malović, T. Makabe, J. de Urquijo, *Appl. Surf. Sci.* **253**, 6619 (2007)
22. J. de Urquijo, J.V. Jovanović, A. Bekstein, V. Stojanović, Z.Lj. Petrović, *Plasma Sources Sci. Technol.* **22**, 025004 (2013)
23. K. Denpoh, K. Nanbu, *J. Vac. Sci. Technol. A* **16**, 1201 (1998)
24. J.B. Hasted, R.A. Smith, *Proc. Roy. Soc. London A* **235**, 349 (1956)
25. C. Lifshitz, *J. Phys. Chem.* **86**, 3634 (1982)
26. F.C. Fehsenfeld, E.E. Ferguson, *J. Chem. Phys.* **61**, 3181 (1974)
27. D. Vogt, *Int. J. Mass. Spectrom. Ion Phys.* **3**, 81 (1969)
28. V. Stojanović, Z. Raspopović, D. Marić, Z.Lj. Petrović, *Contributed Papers, 27th SPIG, Belgrade, August 26–29, 2014*, p. 142
29. J.V. Dugan, J.L. Magee, *J. Chem. Phys.* **47**, 3103 (1967)
30. D.C. Clary, *Chem. Phys. Lett.* **232**, 267 (1995)
31. UMIST RATE12 astrochemistry.net, <http://udfa.ajmarkwick.net/>
32. J.A. de Gouw, M. Krishnamurthy, S.R. Leone, *J. Chem. Phys.* **106**, 5937 (1997)
33. Z.Lj. Petrović, S. Dujko, D. Marić, G. Malović, Ž. Nikitović, O. Šašić, J. Jovanović, V. Stojanović, M. Radmilović-Radenović, *J. Phys. D* **42**, 194002 (2009)
34. R.E. Robson, *Aust. J. Phys.* **44**, 685 (1991)
35. S. Dujko, A.H. Markosyan, R.D. White, U. Ebert, *J. Phys. D* **46**, 475202 (2013)
36. J. de Urquijo, A. Bekstein, G. Ruiz-Vargas, F.J. Gordillo-Vázquez, *J. Phys. D* **46**, 035201 (2013)
37. R.D. White, M.J. Brunger, N.A. Garland, R.E. Robson, K.F. Ness, G. Garcia, J. de Urquijo, S. Dujko, Z.Lj. Petrović, *Eur. Phys. J. D* **68**, 125 (2014)
38. D. Marić, M. Savić, J. Sivoš, N. Škoro, M. Radmilović-Radjenović, G. Malović, Z.Lj. Petrović, *Eur. Phys. J. D* **68**, 155 (2014)